

General Disclaimer

One or more of the Following Statements may affect this Document

- This document has been reproduced from the best copy furnished by the organizational source. It is being released in the interest of making available as much information as possible.
- This document may contain data, which exceeds the sheet parameters. It was furnished in this condition by the organizational source and is the best copy available.
- This document may contain tone-on-tone or color graphs, charts and/or pictures, which have been reproduced in black and white.
- This document is paginated as submitted by the original source.
- Portions of this document are not fully legible due to the historical nature of some of the material. However, it is the best reproduction available from the original submission.

Generated Spiral Bevel Gears: Optimal Machine-Tool Settings and Tooth Contact Analysis

(NASA-TM-87075) GENERATED SPIRAL BEVEL
GEARS: OPTIMAL MACHINE-TOOL SETTINGS AND
TOOTH CONTACT ANALYSIS (NASA) 14 p
HC A02/MF A01 CSCL 13I Unclas
63/37 22216

Faydor L. Litvin and Wei-Jiung Tsung
University of Illinois at Chicago
Chicago, Illinois

John J. Coy
Propulsion Laboratory
AVSCOM Research and Technology Laboratories
Lewis Research Center
Cleveland, Ohio

Charles Heine
Dana Corporation
Fort Wayne, Indiana

Prepared for the
1985 Off-Highway and Power Plant Congress and Exposition
sponsored by the Society of Automotive Engineers
Milwaukee, Wisconsin, September 9-12, 1985



ABSTRACT

Geometry and kinematic errors were studied for Gleason-generated spiral bevel gears. A new method was devised for choosing optimal machine settings. These settings provide zero kinematic errors and an improved bearing contact. The kinematic errors are a major source of noise and vibration in spiral bevel gears. The improved bearing contact gives improved conditions for lubrication. A computer program for tooth contact analysis was developed, and thereby the new generation process was confirmed. The new process is governed by the requirement that during the generation process there is directional constancy of the common normal of the contacting surfaces for generator and generated surfaces of pinion and gear. The process may be imagined as if the generator axes are guided by a parallelogram four-bar linkage.

NOMENCLATURE

$n_f^{(i)}$	unit vector normal to tooth surface ($i = 1, 2$) expressed in coordinate frame S_f .	$n_f^{(i)}$	unit vector normal to tooth surface ($i = 1, 2$) expressed in coordinate frame S_f .
P_1, P_2	main contact points of gear tooth concave and convex sides, respectively (Fig. 6)	P_1, P_2	main contact points of gear tooth concave and convex sides, respectively (Fig. 6)
q_F, q_P	parameters of pinion and gear machine-tool settings (Fig. 3), radians	q_F, q_P	parameters of pinion and gear machine-tool settings (Fig. 3), radians
$r_c^{(F)}, r_c^{(P)}$	theoretical radius of the generating surface measured in plane $x_m^{(i)} = 0$ ($i = 1, 2$) (Fig. 3), cm (in)	$r_c^{(F)}, r_c^{(P)}$	theoretical radius of the generating surface measured in plane $x_m^{(i)} = 0$ ($i = 1, 2$) (Fig. 3), cm (in)
$\Sigma_f^{(i)}$	position vector for a contact point on tooth surface ($i = 1, 2$), expressed in coordinate frame S_f , cm (in)	$\Sigma_f^{(i)}$	position vector for a contact point on tooth surface ($i = 1, 2$), expressed in coordinate frame S_f , cm (in)
u_F, u_P	generating cones surface coordinates (Fig. 3)	u_F, u_P	generating cones surface coordinates (Fig. 3)
b_F, b_P	parameters of pinion and gear machine-tool setting (Fig. 3), cm (in)	$v^{(F)}$	surface Σ_F contact point velocity, cm/sec (in/sec)
$\hat{\lambda}_I^{(1)}, \hat{\lambda}_I^{(2)}$	unit vectors of principal pinion and gear direction (Fig. 8)	$v^{(1)}$	surface Σ_1 contact point velocity, cm/sec (in/sec)
$K_I^{(1)}, K_{II}^{(1)}$	pinion principal curvatures, cm^{-1} (in^{-1})	$2a, 2b$	major and minor axes of contact ellipse (Fig. 8), mm (in)
$K_I^{(2)}, K_{II}^{(2)}$	gear principal curvatures, cm^{-1} (in^{-1})	α	orientation angle of contact ellipse (Fig. 8), radians
m_{12}	gear ratio: $m_{12} = \omega^{(1)} / \omega^{(2)}$	β_F, β_P	pinion, gear spiral bevel angle, degrees
$\tilde{n}^{(F)}$	pinion generator tooth surface unit normal	γ_1, γ_2	pinion, gear pitch angle, degrees
		$\Delta E_1, \Delta L_1$	machine-tool setting corrections (Fig. 5), mm (in)

Δ_1, Δ_2	pinion, gear dedendum angle, degrees
δ	rotation of frame s_h relative to frame S_f about axis Z_1 , radians
δ_e	surface elastic approach, mm (in)
θ_F, θ_P	generating cones surface coordinates (Fig. 3), radians
Σ_1, Σ_2	pinion and gear tooth surfaces
Σ_F, Σ_P	generating surfaces for pinion and gear
$\sigma(21)$	angle formed by unit vectors $i_1^{(2)}$ and $i_1^{(1)}$ (Fig. 8), radians
ϕ_F, ϕ_P	generating surfaces rotation angles (Fig. 3), radians
ϕ_1', ϕ_2'	pinion, gear rotation angle, radians
$\psi_c^{(F)}, \psi_c^{(P)}$	head cutters blade angles for pinion and gear (Fig. 3), degrees
$\omega^{(F)}, \omega^{(P)}$	cradle angular velocities for cutting the pinion and gear, rad/sec
$\omega^{(1)}, \omega^{(2)}$	pinion and gear angular velocities, rad/sec

SUBSCRIPT, SUPERSRIPTS

c	cradle
F	pinion generator
m	machine
P	gear generator
s	surface of generator
1	pinion
2	gear

CARTESIAN COORDINATE FRAMES

$S_c^{(j)}$	connected to cradle
S_f	fixed to frame of gearbox, used for mesh of Σ_1 and Σ_2
S_h	fixed to machine, used for mesh of Σ_F and Σ_1
$S_m^{(i)}$	connected to machine frame $i = 1, 2$
$S_s^{(j)}$	connected to tool cone $j = F, P$

S_1, S_2 connected to pinion, gear

SPIRAL BEVEL GEARS ARE USED in many applications where mechanical power must be transmitted between intersecting drive shafts. Namely, two such applications are the rear axle differential gearbox for land vehicles and the transmissions used in helicopters. For spiral bevel gears, there is a continuing need for ever stronger, lighter weight, longer-lived, and quieter running gears. Above all, a rapid and economical manufacturing method is essential to the industries that use bevel gearing in their products.

For many years, the Gleason Works (1-3)* has provided the machinery for manufacture of spiral bevel gears. There are several important advantages to the Gleason methods of manufacture. The machines are rigid and produce gears of high quality and consistency. The cutting methods may be used for both milling and grinding. Grinding is especially important for producing hardened high quality aircraft gears. Both milling and grinding are possible with Gleason's method since the velocity of the cutting wheel does not have to be related in any way with the machine's generating motions.

A disadvantage is that the Gleason method does not produce conjugate gear tooth surfaces. This means that the gear ratio is not constant during the tooth engagement cycle, and, therefore, there are kinematic errors in the transformation of rotation from the driving gear to the driven gear. On the other hand, it was historically found necessary to provide "mismatch" between the gear tooth surfaces in order to reduce the sensitivity to accidental misalignments during assembly and to the inevitable misalignments caused by gearbox deflections under loaded conditions. The unfortunate byproduct was kinematic error.

The kinematic errors in spiral bevel gears are a major source of noise and vibrations in transmissions. Tests on helicopter transmission vibrations have been conducted by the NASA Lewis Research Center (4). Figure 1 shows the vibration measured by placing an accelerometer on a transmission housing. The bevel gear caused the most noise and vibration. By comparison, the planetary gear stage was relatively quiet.

Therefore, the objective of the research presented herein was to find a way to eliminate the kinematic errors for bevel gears, while retaining all the advantages of the Gleason system of manufacturing such gears. The gear cutting machines have a number of special settings called "machine settings" which uniquely determine the motion characteristics of the manufactured gears. There are many combinations of machine settings that will produce the same nominal gear. Within such an allowable group of machine settings there is an optimum combination that will give zero kinematic errors.

*Numbers in parentheses designate references at end of paper.

The methods for determining these settings are described in this paper. The main feature of the modified gearing is that the contact normal to the gear tooth surfaces does not change its direction in the process of meshing.

In addition several other important features of previous research on bevel gears are included in this research. Litvin and his colleagues have addressed the analysis and synthesis of spiral bevel gears (5-8). Computer aided simulations of the conditions of tooth meshing and bearing contact have been worked out by Litvin and Gutman (9,10) and by the Gleason Works (2,3). The so-called tooth "bearing" contact is the envelope of the contact ellipses between the gear teeth as they go through the mesh cycle. The best bearing contact moves lengthwise along the tooth rather than along a line between the root and tip of the tooth. This type of motion gives improved conditions for lubrication.

The key features and principal equations of the methods of analysis and synthesis are presented herein. Not all details are given due to limited space. The results presented herein are based on a new tooth contact analysis (TCA) computer program using the new methods of synthesis.

MANUFACTURING METHOD

The gear cutter cuts a single space during a single index cycle. The gear cutter is mounted to the cradle of the cutting machine. The cutter spins about an axis which itself moves in a circular path. At the same time, the gear blank rotates. The combined process generates the gear tooth. The machine cradle with the gear cutter may be imagined as a crown gear that meshes with the gear being cut. The cradle rotates slowly about its axis, as does the gear which is being cut. The cutter spins rapidly. The cradle only rotates far enough so that one tooth is cut and then it rapidly reverses while the workpiece is withdrawn from the cutter and indexed ahead in preparation for cutting the next tooth.

We consider that two generating surfaces, Σ_F and Σ_P , are used for the generation of the pinion tooth surface, Σ_1 , and the gear tooth surface, Σ_2 , respectively. The flanks of adjacent teeth are cut simultaneously (duplex method) but each side of the pinion tooth is cut separately. The basic machine-tool settings provide that four surfaces, Σ_F , Σ_P , Σ_1 , and Σ_2 , are in contact at the main contact point. In the process of meshing, surfaces Σ_F and Σ_1 , and respectively surfaces Σ_P and Σ_2 contact each other at every instant at a line (contact line) which is a spatial curve. The shape of the contact line and its location on the contacting surfaces is changed in the process of meshing. The generated pinion and gear tooth surfaces are in contact at a point (contact point) at every instant.

A head-cutter used for the gear generation is shown in Fig. 2. The shapes of the blades

of the head-cutter are straight lines which generate a cone while the head-cutter rotates about axis C-C. The angular velocity about axis C-C does not depend on the generation motion but only on the desired cutting velocity. Two head-cutters are used for the pinion generation; they are provided with one-sided blades and cut the respective tooth sides separately. The head cutter is mounted to the cradle of the machine.

Figure 3 shows the cone-surface which is the generating tool surface. We consider two coordinate systems rigidly connected to the cradle: (1) $S_c^{(j)}$ in which we represent the cone surface and (2) $S_g^{(j)}$ which is rigidly connected to $S_c^{(j)}$ and rotates about the $x_m^{(i)}$ -axis of the fixed coordinate systems $S_m^{(i)}$ ($j = F, P; i = 1, 2$ see nomenclature). The cradle with the cone surface represents the generating gear which is in mesh with the pinion (gear) in the process of cutting. The cone surface represents the surface of the tooth-side surface of the generating gear.

The generating surfaces are represented in $S_c^{(j)}$ ($j = F, P$) by the following equations:

$$\begin{aligned} x_c^{(j)} &= r_c^{(j)} \cot \psi_c^{(j)} - u_j \cos \psi_c^{(j)} \\ y_c^{(j)} &= u_j \sin \psi_c^{(j)} \sin (\theta_j \mp q_j) \mp b_j \sin q_j \\ z_c^{(j)} &= u_j \sin \psi_c^{(j)} \cos (\theta_j \mp q_j) + b_j \cos q_j \end{aligned} \quad (j = F, P) \quad (1)$$

where u_j, θ_j are the coordinates of a point on the tool cone surface (generating surface); b_j and q_j are the parameters of machine-tool settings; $r_c^{(j)}$ is the head-cutter radius which is measured in plane $x_m^{(i)} = 0$; and the upper and lower signs for q_j in Eqs. (1) are given for the right-hand spiral and left-hand spiral gears, respectively.

The cradle of the cutting machine carries the head-cutter (Fig. 4). The cradle rotates about the $x_m^{(2)}$ coordinate axis with angular velocity $\omega^{(P)}$ while the gear being generated rotates about its axis Z_2 with angular velocity $\omega^{(2)}$. The angular velocities of cradle and gear are related by ratio $m_{2P} = \omega^{(2)}/\omega^{(P)}$. Axis $x_m^{(2)}$ is perpendicular to the element of the gear root cone as shown in Fig. 4. Thus, axes Z_2 and $Z_m^{(2)}$ make the angle $\gamma_2 - \Delta_2$, where γ_2 is the pitch angle and Δ_2 is the gear dedendum angle.

An auxiliary fixed coordinate system S_f is rigidly connected to the housing of the gear train. We will consider the meshing of gears 1 and 2 in system S_f .

GENERATING THE GEAR - Considering the generation of gear 2 (Fig. 4), we use the following coordinate systems: (1) $S_c^{(P)}$, a movable coordinate system, which is rigidly connected to the generating gear (to the cradle with the

generating surface Σ_P) and (2) a fixed coordinate system $S_m^{(2)}$ which is rigidly connected to the frame of the cutting machine, and the coordinate system S_2 which is rigidly connected to gear 2. The location of coordinate system $S_s^{(F)}$ with respect to $S_c^{(F)}$ is determined by q_P and b_P (Fig. 3). ϕ_P represents the cradle rotation, $r_c^{(F)}$ is the radius of the head cutter circle, and β_P is the root cone spiral angle.

GENERATING THE PINION - Similarly, considering the pinion generation, we use the coordinate systems $S_s^{(F)}$ (Fig. 3), $S_c^{(F)}$, $S_m^{(1)}$, and S_1 (Fig. 5). We designate S_h to be an auxiliary fixed coordinate system, where we consider the mesh of surfaces Σ_F and Σ_1 . Coordinate systems S_h and S_f are related by having a common origin and a small relative angular displacement. Unlike for the generation of gear 2, the axes of rotation $x_m^{(1)}$ and Z_1 do not intersect each other; rather they cross. It is necessary to introduce this crossing of axes in order to gain degrees of freedom in designing the cutting process and allowing the possibility to minimize the kinematic errors. ΔE_1 and ΔL_1 are the sought-for corrections of the machine-tool settings with which the meshing of gears 1 and 2 is to be improved. In addition, two other parameters must be determined. They are the blade angle $\psi_c^{(F)}$ and a turning angle δ . Angle δ determines the orientation of coordinate frame S_h with respect to S_f . This turning is performed about the pinion axis, Z_1 , when the gear and pinion will have been placed in mesh and with the origins O_h and O_f being coincident.

DERIVATION OF NEW SETTINGS (SYNTHESIS)

Deriving the machine-tool settings, we have to satisfy the following requirements: (1) the generating surfaces, Σ_F and Σ_P , and the gear tooth surfaces, Σ_1 and Σ_2 , must be in contact at the main contact point. The main contact points for the gear tooth concave and convex sides are P_1 and P_2 , respectively (Fig. 6); (2) the cutting ratio for the gear generation provides that the instantaneous axis of rotation by the gear cutting coincides with the pitch line O_fP (Fig. 6); (3) the cutting ratio for the pinion generation provides that the equation of meshing for surfaces Σ_F and Σ_1 is satisfied at the main contact point. The equation of meshing is given by

$$\underline{n}^{(F)} \cdot \underline{v}^{(F1)} = 0 \quad (2)$$

Here $\underline{n}^{(F)}$ is the unit normal to the generating surface Σ_F ; $\underline{v}^{(F1)} = \underline{v}^{(F)} - \underline{v}^{(1)}$ where $\underline{v}^{(F)}$ and $\underline{v}^{(1)}$ are the velocities of the point of tangency of surfaces Σ_F and Σ_1 , respectively; (4) the blade angle for the gear head-cutter is considered as given; the blade angle for the pinion has to satisfy the requirement that the generating surfaces, Σ_F and Σ_P , have a common normal at the main contact point; and

(5) the gear ratio is given by $m_{12}(\phi_1) = \omega^{(1)}/\omega^{(2)}$ where ϕ_1 is the gear angle rotation and $\omega^{(1)}$ and $\omega^{(2)}$ are the rotational speeds of pinion and gear.

Equations were written to represent the above conditions in a computer program for the purpose of iteratively seeking the values of ΔE_1 , ΔL_1 , $\psi_c^{(F)}$ and δ that would minimize the kinematic error. The starting point is to require that

$$\frac{dm_{12}(\phi_1)}{d\phi_1} = 0 \quad (3)$$

at the main contact point.

The result of the analysis requires that the following relation is satisfied.

$$\Delta E_1 \cos \tau_F = \Delta L_1 \sin \tau_F \quad (4)$$

where

$$\tau_F = \theta_F + q_F + \phi_F \quad (5)$$

and θ_F is the surface coordinate of the generating cone determined for the main contact point; q_F is the setting parameter (Fig. 3); and the upper and lower signs for q_F in Eqs. (5) and (1) are given for the right-hand spiral and left-hand spiral gears, respectively.

To help in a physical understanding of the theoretical result, consider Fig. 7. A feature of the theoretical result is that, during the entire process of meshing, the special machine settings provide a constant direction of the contact normal to the gear tooth surfaces. We may interpret the new process of gear generation as described in Fig. 7, which applies in the neighborhood of the main contact point. Imagine that the four involved surfaces Σ_1 , Σ_2 , Σ_F and Σ_P are in continuous contact, with the centers of tool cones Σ_F and Σ_P carried on a parallelogram linkage.

The drawing shown in Fig. 7 is presented in plane Π which is drawn through the common normal to the gear tooth surfaces (C_iP , $i = 1, 2$) and the instantaneous axis of rotation of the gear (O_2P). The generating surfaces Σ_F and Σ_P are in contact at P . Curves L_F and L_P are obtained by the intersection of plane Π with the generating surfaces Σ_F and Σ_P . The difference of curvature radii $\rho_c^{(P)}$ and $\rho_c^{(F)}$ provides the desired localization of bearing contact.

We may imagine that both generating surfaces are carried by the connecting rod of the parallelogram $O_2C_1C_1C_2$. The generating surface rotates about an axis which intersects plane Π at point O_i ($i = 1, 2$). Thus, point O_i is the center of rotation of the crank of the parallelogram. It is evident that the common normal to the generating surfaces will keep its original direction within the neighborhood of the main contact point P .

since the connecting rod performs a curvilinear translational motion.

TOOTH CONTACT ANALYSIS

KINEMATIC ERROR - A tooth contact analysis computer program was developed to provide numerical results that check the theory that was derived to minimize the kinematic errors. The TCA program calculates tooth bearing contact, contact path, and kinematic errors as a result of the input, which includes the machine settings. The program is based on the following principle. At the instantaneous contact point between the meshing teeth, the position vectors must agree, the equations for meshing between generator and generated gear must be obeyed, and the surface normals must agree. The following equations represent these principles.

$$\vec{r}_f^{(1)}(u_F, \theta_F, \phi_F, \phi_1') = \vec{r}_f^{(2)}(u_P, \theta_P, \phi_P, \phi_2') \quad (6)$$

$$f_F(u_F, \theta_F, \phi_F) = 0 \quad (7)$$

$$f_P(u_P, \theta_P, \phi_P) = 0 \quad (8)$$

$$\vec{R}_f^{(1)}(\theta_F, \phi_F, \phi_1') = \vec{R}_f^{(2)}(\theta_P, \phi_P, \phi_2') \quad (9)$$

Here, ϕ_1' and ϕ_2' are the angles of rotation of gears 1 and 2, respectively, when they are in mesh; ϕ_F and ϕ_P are the angles of rotation of the generating gears.

The equations of meshing (7) and (8) are linear in u_F and u_P respectively. Eliminating u_F and u_P , we may represent Eqs. (6) to (8) as follows:

$$\vec{r}_f^{(1)}(\theta_F, \phi_F, \phi_1') = \vec{r}_f^{(2)}(\theta_P, \phi_P, \phi_2') \quad (10)$$

Equations (9) and (10), considered simultaneously, express that when surfaces Σ_1 and Σ_2 are in mesh, they have a common point and a common normal, and that such a point is the contacting point of the gear tooth surface. Since Eqs. (9) and (10) are vector equations, there are a total of six scalar equations. Because the surface normal vectors are unit vectors, there are only five independent scalar equations in six unknowns. Fixing one of the six unknowns in these equations (say θ_F), we may solve the system for the other parameters as functions of θ_F . This may be represented as follows:

$$\begin{aligned} &\theta_P(\theta_F), \phi_F(\theta_F), \phi_P(\theta_F) \\ &\phi_1'(\theta_F), \phi_2'(\theta_F) \end{aligned} \quad (11)$$

The equations are solved using a nonlinear equation solver which is based on an iterative

scheme. The kinematic errors are determined simply by comparing the rotations ϕ_1 and ϕ_2 .

BEARING CONTACT - The determination of the dimensions and orientation of the contact ellipse at the contacting point is based on the method developed by Litvin (5,6,11). The method starts with the equation for the normal curvature which comes from differential geometry theory.

$$K_n = \frac{\ddot{n} \cdot \dot{v}}{v^2} \quad (12)$$

where K_n is the normal curvature, \dot{v} is the velocity of the contact point across the surface and \ddot{n} is the velocity of the tip of the surface unit normal, \dot{n} , which changes its direction while the point moves over the surface.

The method of finding the contact ellipse is further developed by the following considerations in solving a characteristic value (eigenvalue) problem. The maximum and minimum values of curvature are the "principal" values of curvature and the principal directions are the corresponding directions of the unit vectors that are tangent to the line of intersection formed by the normal plane and the surface whose curvature is sought. The method is to determine the principal curvatures and directions of surfaces Σ_1 and Σ_2 in terms of the principal curvatures and directions of the generating surfaces Σ_F and Σ_P . Then the relations between the principal curvatures and direction of the contacting surfaces are used to determine the contact ellipse of the elastically deformed tooth surfaces.

Consider that the principal curvatures and directions for the contacting surfaces are determined and A (Fig. 8) is the point of contact of gear tooth surfaces and the unit vectors $\dot{i}_1^{(2)}$ and $\dot{i}_1^{(1)}$ represent principal directions $I^{(i)}$ on gear tooth surfaces, Σ_1 and Σ_2 . Principal direction $II^{(i)}$ is perpendicular to the unit vector $\dot{i}_1^{(i)}$ ($i = 1, 2$). Unit vectors $\dot{i}_1^{(2)}$ and $\dot{i}_1^{(1)}$ lie in the tangent plane to surfaces Σ_2 and Σ_1 which is drawn through the instantaneous contact point A. Angle σ (21) which is formed by unit vectors $\dot{i}_1^{(2)}$ and $\dot{i}_1^{(1)}$ is known since the principal directions for the mating surfaces have already been determined.

Axes 2a and 2b of the contact ellipse represent its dimensions and angle σ its orientation with respect to $\dot{i}_1^{(2)}$. Angle α is measured counter-clockwise from the η -axis to $\dot{i}_1^{(2)}$. We may determine a, b and α using the following equations (11):

$$A = \frac{1}{4} \left[K_c^{(1)} - K_c^{(2)} - \left(g_1^2 - 2g_1g_2 \cos 2\sigma \right)^{1/2} + g_2^2 \right] \quad (13)$$

$$B = \frac{1}{4} \left[K_c^{(1)} - K_c^{(2)} + \left(g_1^2 - 2g_1g_2 \cos 2\alpha \right. \right. \\ \left. \left. + g_2^2 \right)^{1/2} \right] \quad (14)$$

$$a = \left(\left| \frac{\delta_e}{A} \right| \right)^{1/2}, \quad b = \left(\left| \frac{\delta_e}{B} \right| \right)^{1/2} \quad (15)$$

$$\tan 2\alpha = \frac{g_2 \sin 2\sigma}{g_1 - g_2 \cos \sigma} \quad (16)$$

where

$$K_c^{(i)} = K_{I}^{(i)} + K_{II}^{(i)}, \quad \text{and} \quad g_i = K_{I}^{(i)} \\ - K_{II}^{(i)} \quad (i = 1, 2) \quad (17)$$

δ_e is the approach of the elastic surfaces under the load. The ratio of ellipse axes is represented as follows:

$$\frac{a}{b} = \left| \frac{B}{A} \right| \quad (18)$$

The bearing contact is simply the envelope of the set of contact ellipses for whole meshing cycle of the mating teeth.

NUMERICAL EXAMPLE - Figure 9 shows the bearing contact on the convex side of the gear tooth in a set of bevel gears with the following parameters:

Tooth numbers,

$$N_1 = 10, \quad N_2 = 41$$

Gear pressure angle,

$$\psi_c^{(P)} = 20^\circ$$

Diametral pitch,

$$P_d = 141.2 \text{ mm (5.559 in)}$$

Mean cone pitch distance,

$$O_h N = 81.94 \text{ mm (3.226 in)}$$

Cutter diameter,

$$r_c^{(P)} = 76.20 \text{ mm (3.000 in)}$$

and

$$\Delta L_1 = -1.27 \text{ mm (-0.0499 in)}$$

$$\Delta L_2 = -0.93 \text{ mm (-0.0368 in)}$$

The contact ellipse moves along the surface in the process of meshing. The kinematic error is zero over the whole mesh cycle if the pinion

cutter blade angle, $\psi_c^{(F)} = 16.969^\circ$ and $\delta = -0.274^\circ$. However this blade angle is not practical. Choosing the nearest blade angle $\psi_c^{(F)} = 17^\circ$ requires also that $\delta = -0.314^\circ$ and hence results in nonzero kinematic errors, but they are still very small. For this example, they are less than 0.02 arc sec. For gears made without the special machine settings, the kinematic errors are in the range from 20 to 90 arc sec.

SUMMARY OF RESULTS

Spiral bevel gear geometry was investigated using the standard laws of kinematics for spatial gearings, as well as important results from the differential geometry field. The object was to eliminate kinematic errors in the motion transmission because such errors are a major source of noise and vibration. A computer program was created that simulates the cutting and meshing processes for the pinion and gear. The computer program yielded the tooth geometry, contact path, kinematic errors, and contact ellipse between the mating gear teeth.

The following results were obtained.

1. A method of generating spiral bevel gears with zero kinematical errors was developed. Gleason gear generating equipment may be used. Practical considerations of using standard blade angles give nonzero but still very small kinematic errors.
2. The generation process takes place under the requirement of a constant direction for the contact normal during the process of meshing. The process may be imagined as if the tool cone centers are carried on a parallelogram four-bar linkage during the tooth generation process.
3. The new process provides that the contact ellipse moves lengthwise along the tooth in the most advantageous way for good lubrication.
4. The new generation method was confirmed by calculations run on a digital computer program for tooth contact analysis.

REFERENCES

1. D.W. Dudley, "Bevel and Hybrid Gear Manufacture," Chapter 20 of Gear Handbook: The Design, Manufacture, and Application of Gears by D.W. Dudley. New York: McGraw-Hill, 1962.
2. "Tooth Contact Analysis, Formulas, and Calculation Procedures," Distributed by Gleason Machine Division, The Gleason Works, 1000 University Avenue, Rochester, NY 14692. Publication No. SD3115, 1964.

3. "Understanding Tooth Contact Analysis.." Distributed by Gleason Machine Division, The Gleason Works, 1000 University Avenue, Rochester, NY 14692. Publication No. SD3139, c1981.
4. D.P. Townsend, J.J. Coy, and B.R. Hatvani, "OH-58 Helicopter Transmission Failure Analysis," NASA TM-X-71867, January, 1976.
5. F.L. Litvin, "The Theory of Gearing," 2d ed. Moscow: Nauka, 1968.
6. F.L. Litvin, P. Rahman, and R.N. Goldrich, "Mathematical Models for the Synthesis and Optimization of Spiral Bevel Gear Tooth Surfaces for Helicopter Transmissions," NASA CR-3553, June, 1982.
7. F.L. Litvin and J.J. Coy, "Spiral-Bevel Geometry and Gear Train Precision," in Advanced Power Transmission Technology. Cleveland, OH: NASA Lewis Research Center, 1983, NASA CP-2210, AVRADCOM TR 82-C-16 pp. 335-344.
8. F.L. Litvin, M.S. Hayasaka, P. Rahman, and J.J. Coy, "Synthesis and Analysis of Spiral Bevel Gears," in Design and Synthesis: Proceedings of the International Symposium on Design and Synthesis, Tokyo, Japan, July 11-13, 1984 ed. by H. Yoshikawa. New York: North Holland, 1985, pp. 302-305.
9. F.L. Litvin and Y. Gutman, "Methods of Synthesis and Analysis for Hypoid Gear-Drives of "Formate" and "Helixform," Parts 1-3, Transactions of the ASME: Journal of Mechanical Design, Vol. 103, January 1981, pp. 83-113.
10. F.L. Litvin and Y. Gutman, "A Method of Local Synthesis of Gears Grounded on the Connections between the Principal and Geodesic Curvatures of Surfaces," Transactions of the ASME: Journal of Mechanical Design, Vol. 103, January 1981, pp. 114-125.
11. F.L. Litvin, "Relationships between the Curvatures of Tooth Surfaces in Three-Dimensional Gear Systems," NASA-TM-75130, July, 1977.

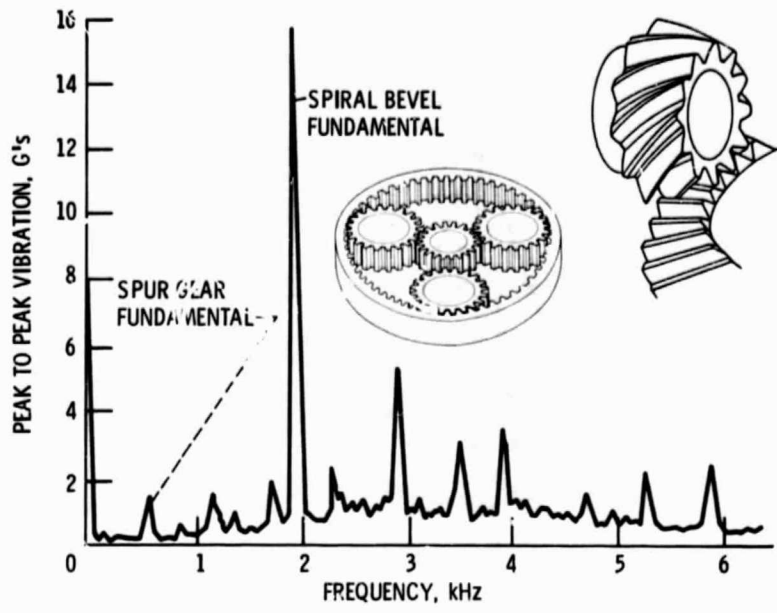


Figure 1. - Transmission vibration spectrum.

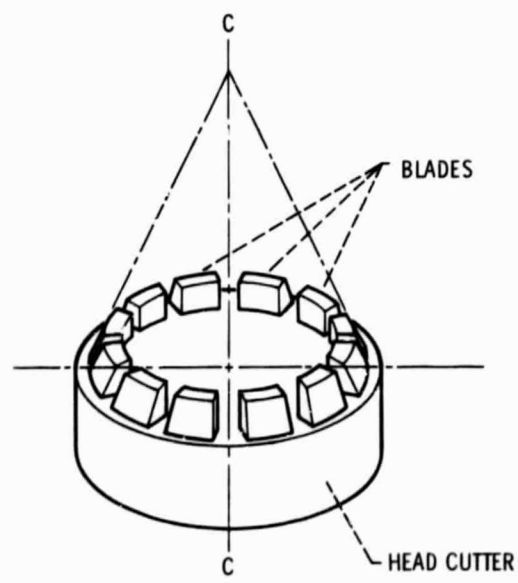
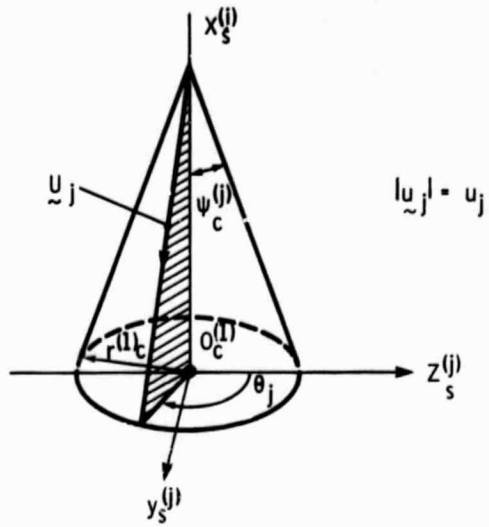
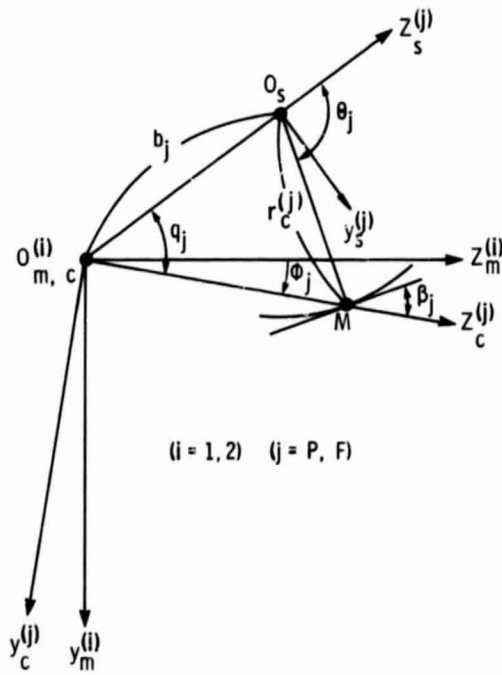


Figure 2. - Cutting tool.



(a) Tool cone.



(i = 1, 2) (j = P, F)

(b) Machine plane.

Figure 3. - Machine settings.

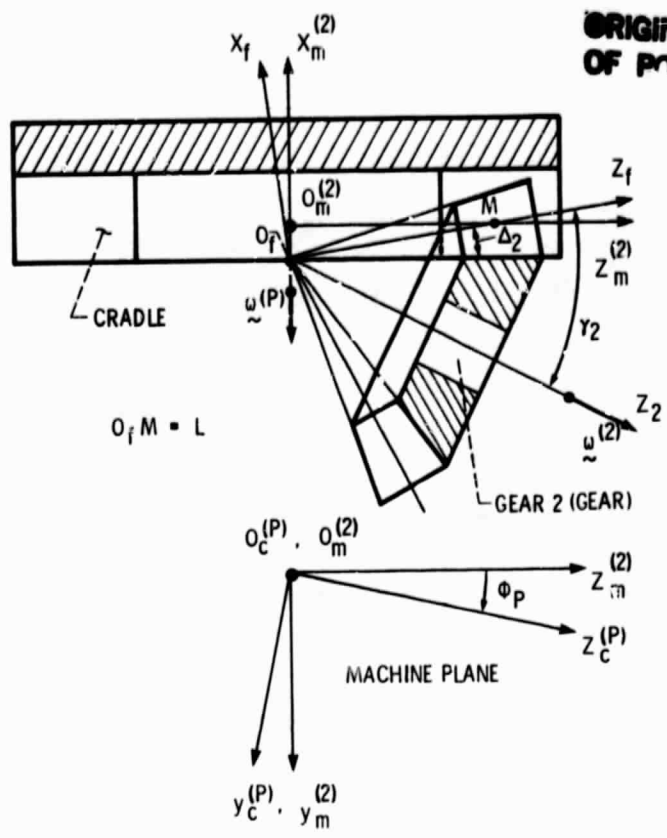


Figure 4. - Gear generation.

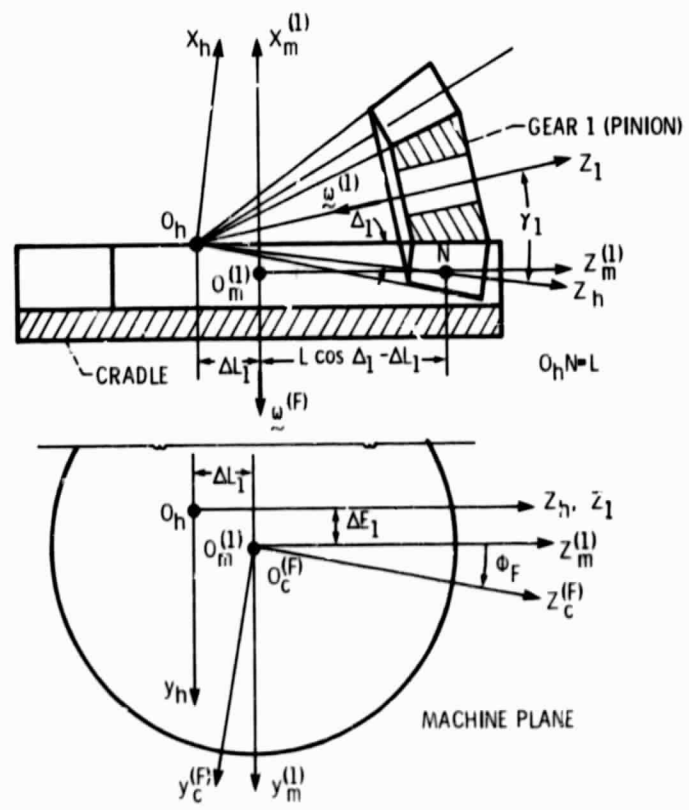


Figure 5. - Pinion generation.

ORIGINAL PAGE IS
OF POOR QUALITY

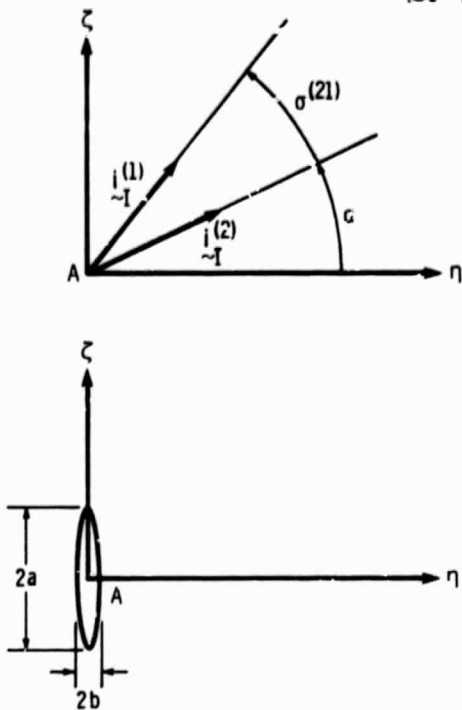


Figure 8. - Contact ellipse and principal directions.

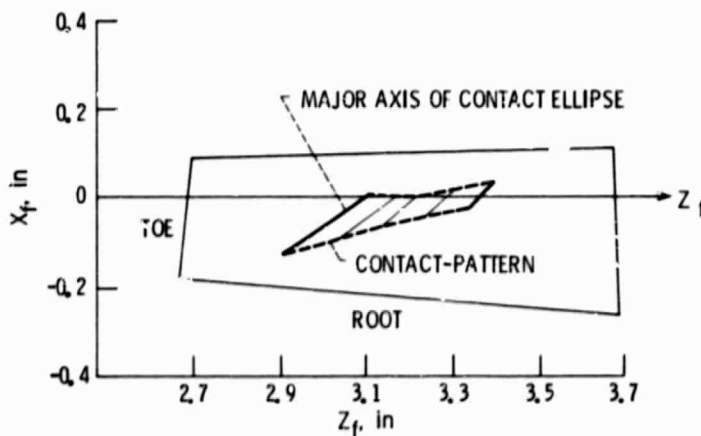


Figure 9. - Contact pattern - the envelope of contact ellipses,
 $\psi_c^{(P)} = 20^\circ$; $\psi_c^{(F)} = 17^\circ$; convex side of tooth.

1. Report No. NASA TM-87075 USAAVSCOM-TR-85-C-9		2. Government Accession No.		3. Recipient's Catalog No.	
4. Title and Subtitle Generated Spiral Bevel Gears: Optimal Machine-Tool Settings and Tooth Contact Analysis				5. Report Date	
				6. Performing Organization Code 505-42-94	
7. Author(s) Faydor L. Litvin, Wei-Jiung Tsung, John J. Coy, and Charles Heine				8. Performing Organization Report No. E-2648	
				10. Work Unit No.	
9. Performing Organization Name and Address NASA Lewis Research Center and Propulsion Laboratory U.S. Army Research and Technology Laboratories (AVSCOM) Cleveland, Ohio 44135				11. Contract or Grant No.	
				13. Type of Report and Period Covered Technical Memorandum	
12. Sponsoring Agency Name and Address National Aeronautics and Space Administration Washington, D.C. 20546 and U.S. Army Aviation Systems Command, St. Louis, Mo. 63120				14. Sponsoring Agency Code	
15. Supplementary Notes Faydor L. Litvin and Wei-Jiung Tsung, University of Illinois at Chicago, Chicago, Illinois (work performed under NASA Grant NSG 3-48); John J. Coy, Propulsion Laboratory, AVSCOM Research and Technology Laboratories, Lewis Research Center, Cleveland, Ohio; Charles Heine, Dana Corporation, Fort Wayne, Indiana. Prepared for the 1985 Off-Highway and Power Plant Congress and Exposition, sponsored by the Society of Automotive Engineers, Milwaukee, Wisconsin, September 9-12, 1985.					
16. Abstract Geometry and kinematic errors were studied for Gleason-generated spiral bevel gears. A new method was devised for choosing optimal machine settings. These settings provide zero kinematic errors and an improved bearing contact. The kinematic errors are a major source of noise and vibration in spiral bevel gears. The improved bearing contact gives improved conditions for lubrication. A computer program for tooth contact analysis was developed, and thereby the new generation process was confirmed. The new process is governed by the requirement that during the generation process there is directional constancy of the common normal of the contacting surfaces for generator and generated surfaces of pinion and gear. The process may be imagined as if the generator axes are guided by a parallelogram four-bar linkage.					
17. Key Words (Suggested by Author) Spiral bevel gears; Mechanisms; Vibrations; Machine designs			18. Distribution Statement Unclassified - unlimited STAR Category 37		
19. Security Classif. (of this report) Unclassified		20. Security Classif. (of this page) Unclassified		21. No. of pages	22. Price*